Porphyrins Hot Paper

International Edition: DOI: 10.1002/anie.201511981
German Edition: DOI: 10.1002/ange.201511981

Directly Diphenylborane-Fused Porphyrins

Keisuke Fujimoto, Juwon Oh, Hideki Yorimitsu, Dongho Kim,* and Atsuhiro Osuka**

Abstract: *Mono- and bis(diphenylborane)-fused porphyrins were synthesized from the corresponding β-(2-trimethylsilylphenyl)-substituted porphyrins through the sequence of Si–B exchange reaction, intramolecular bora-Friedel–Crafts reaction, and ring-closing Si–B exchange reaction. Effective electronic interactions of the empty p-orbital of the boron atom with the porphyrin π-circuit lead to red-shifted absorption spectra and substantially decreased LUMO energy levels. Pyridine adds at the boron center to cause disruption of the electronic interaction of the boron atom with large association constants ($1.9–17\times10^4\,M^{-1}$) depending on the central metal at the porphyrin. The Zn^{II} complex behaved as a hetero-dinuclear Lewis acid, exhibiting regioselective binding of pyridines at the boron or the zinc center.*

Hybrids of porphyrin and triorganoborane are expected to be promising functional molecules since porphyrins have rich optical, electrochemical, and coordination properties, and these properties should be strongly perturbed through effective interactions with the empty p-orbital of the boron atom. Along this line, we recently synthesized dimesitylporphyrinylboranes for the first time by reactions of porphyrinyllithiums with dimesitylfluoroborane.[1] While the porphyrinylboranes are kinetically stable owing to the steric protection of the large aryl groups, they display only marginally perturbed optical and electrochemical properties because of their twisted conformations. To enhance electronic interactions between a porphyrin and a boron atom, we envisioned diphenylborane-fused porphyrins **1M** and **2Ni** (Scheme 1), in which the *meso*-boron atom is embedded in a fused skeleton to force the p-orbital of the boron atom to strongly interact with the π-electronic network of the porphyrin. The target diphenylborane-fused porphyrins can be regarded as "structurally constrained" triarylboranes, which have high chemical stabilities and undergo reversible coordination with strong Lewis bases resulting in alternation of the structural and electronic properties.[2]

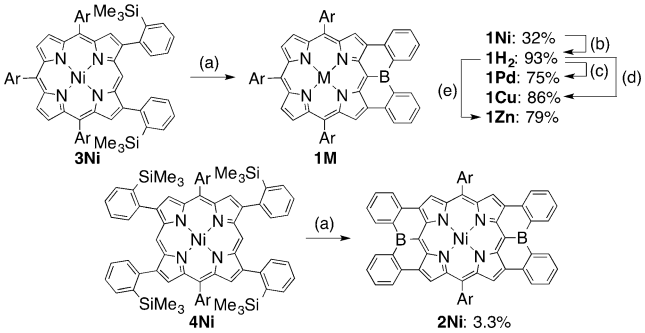

Scheme 1. Synthesis of diphenylborane-fused porphyrins **1M** (M = metal) and **2Ni** (Ar = 3,5-di-*tert*-butylphenyl). a) BBr_3, *o*-dichlorobenzene, 80 °C; b) $TFA/H_2SO_4/CH_2Cl_2$, 0 °C; c) $PdCl_2(PhCN)_2$, PhCN, 140 °C; d) $Cu(OAc)_2$, CH_2Cl_2/MeOH, room temperature; e) $Zn(OAc)_2\cdot H_2O$, CH_2Cl_2/MeOH, room temperature.

A simple synthetic route to **1M** would involve an initial installation of a boron atom at the *meso*-position and a subsequent oxidative fusion reaction.[3] However, such an oxidative route is not suitable for the synthesis of **1M** because a required intermediate, *meso*-diphenylborylporphyrin, would be unstable even under ambient conditions. Hence, we designed a new synthetic route toward **1Ni** via the key intermediate **3Ni** bearing an unsubstituted *meso*-position and two trimethylsilylphenyl groups (Scheme 1). One of the trimethylsilyl groups in **3Ni** is convertible into a BBr_2 group by an Si–B exchange reaction with BBr_3[4] and then the second C–B bond can be formed by an intramolecular bora-Friedel–Crafts reaction[5] at the nucleophilic *meso*-carbon atom. Finally, a ring-closing Si–B exchange reaction at the other trimethylsilyl group should furnish **1Ni** (see Scheme S1 in the Supported Information for detailed plausible mechanism).

Porphyrin **3Ni** was synthesized from 3,7-diiodoporphyrin[6] by Negishi cross-coupling reaction with 2-trimethylsilylphenylzinc chloride[7] in the presence of a $Pd_2(dba)_3$/2-dicyclohexylphosphino-2′,6′-diisopropoxybiphenyl (Ruphos) catalysis.[8] Indeed, the designed one-pot borylation proceeded efficiently by treatment of **3Ni** with BBr_3 to give diphenylborane-fused porphyrin **1Ni** in 32% yield. Compound **1Ni** is stable toward moisture, oxygen, and silica gel, which allowed for its separation without any special measures. To our surprise, the C–B bonds of **1Ni** are stable even under strongly acidic conditions, which enabled its denickelation in $CH_2Cl_2/TFA/H_2SO_4$ to afford free-base porphyrin **$1H_2$** in 93% yield. Further metalation of **$1H_2$** provided palladium, copper, and zinc complexes **1Pd**, **1Cu**, and **1Zn** in good yields, respectively. Stable bis(diphenylborane)-fused porphyrin **2Ni** was also synthesized from **4Ni** in a similar fashion in 3.3% yield.

All the structures of **1Ni**, **$1H_2$**, **1Pd**, **1Cu**, and **1Zn** were revealed by X-ray crystallographic analysis (Figure 1 and

[*] K. Fujimoto, Prof. Dr. H. Yorimitsu, Prof. Dr. A. Osuka
Department of Chemistry, Graduate School of Science
Kyoto University
Sakyo-ku, Kyoto 606–8502 (Japan)
E-mail: yori@kuchem.kyoto-u.ac.jp
osuka@kuchem.kyoto-u.ac.jp
J. Oh, Prof. Dr. D. Kim
Spectroscopy Laboratory of Functional π-Electronic Systems and Department of Chemistry
Yonsei University
Seoul 120–749 (Korea)
E-mail: dongho@yonsei.ac.kr

Supporting information for this article is available on the WWW under http://dx.doi.org/10.1002/anie.201511981.

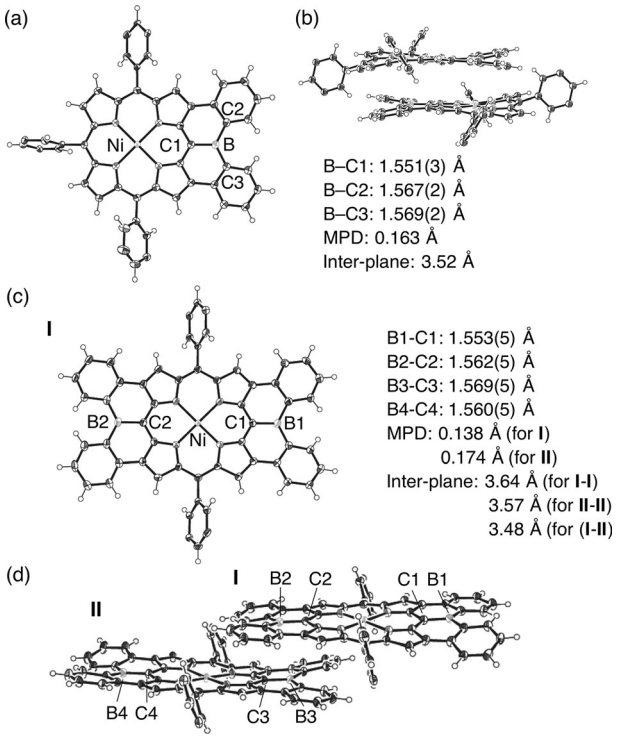

Figure 1. X-Ray crystal structures of **1Ni**, a) top view and b) side view, and **2Ni**, c) top view and d) side view. Independent two molecules in an asymmetric unit are shown for (d). Thermal ellipsoids set at 50% probability. Solvent molecules and *tert*-butyl groups are omitted for clarity.

Figure S22, S23, and S24). Two porphyrin molecules are stacked in an antiparallel face-to-face arrangement in the crystals with inter-plane distances of 3.52–3.62 Å, which are in the range of typical π–π stacking. The sums of three ∡CBC angles are almost 360°, indicating the strict planar tricoordinate geometries of the boron atoms. The B–C1 bonds are 1.551(3) 1.546(5), 1.549(5), 1.546(3), and 1.527(9) Å for **1Ni**, **1H$_2$**, **1Pd**, **1Cu**, and **1Zn**, respectively, which are significantly shorter than the other B–C2 and B–C3 bonds (1.561–1.576 Å), and typical B–C(aryl) bond length (1.58 Å),[9] suggesting a structural constraint and an increase of the bond order in the B–C1 bond. The diphenylborane moieties are helically twisted because of the steric repulsion of the hydrogen atoms close to the boron atom. The porphyrin moiety of **1Ni** takes a saddle conformation as often seen in Ni^{II} porphyrins[10] with a mean plane deviation (MPD) value[11] of 0.163 Å. In contrast, **1Cu** shows a smaller MPD value (0.042 Å) indicating a rigid planar structure of **1Cu** as is typical for Cu^{II} porphyrins.[10]

The X-ray crystallographic analysis of **2Ni** revealed two independent molecules **I** and **II** that are arranged pairwise as an offset step-like packing structure (Figure 1, and Figure S24). The MPD values are 0.138 and 0.174 Å for **I** and **II**, and the interporphyrin distances are 3.64 Å for **I–I**, 3.57 Å for **II–II**, and 3.48 Å for **I–II**. Similar to **1Ni**, the B-C(*meso*) bond length of **2Ni** are 1.553(5), 1.562(5), 1.569(5), and 1.560(5) Å, which are shorter than those of the B–C(Ph) bonds (1.569 Å (average of the eight bonds)).

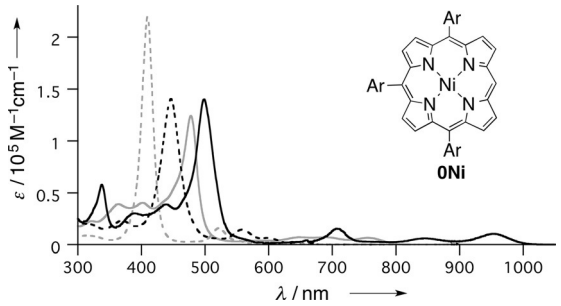

Figure 2. UV/Vis absorption spectra of **0Ni** (gray, dashed), **1Ni** (gray), **1Ni·py** ([**1Ni**]$_0$: 5.0 μM, [pyridine]: 0.15 mM, black, dashed), and **2Ni** (black) in CH_2Cl_2.

The absorption spectrum of **1Ni** is significantly red-shifted from that of the reference porphyrin **0Ni**, showing a Soret band at 478 nm and Q bands at 649, 689, and 755 nm (Figure 2). The absorption spectra of **1H$_2$**, **1Pd**, **1Cu**, and **1Zn** are similar to that of **1Ni** (see Figure S26). The observed spectral red-shifts can be ascribed to the electronic interactions between the fused diphenylborane group and the porphyrin π-network. Bis(diphenylborane)-fused **2Ni** shows a further red-shifted spectrum displaying a Soret band at 499 nm and Q bands at 706, 845, and 956 nm, suggesting further extension of π-network. Addition of pyridine to a solution of **1Ni** caused distinct blue shifts, showing a Soret band at 446 nm and Q bands at 558 and 596 nm. **1H$_2$**, **1Pd**, and **1Cu** exhibit spectral blue-shifts upon addition of pyridine in a manner similar to that of **1Ni** (see Figure S27). These spectral characteristics indicate the formation of pyridine complex **1M·py** (see below).

Electrochemical studies also revealed strong perturbation of the porphyrinic electronic system by the fused boron moieties (see Figure S36). The first reduction potentials of **1Ni** and **2Ni** were observed at −1.20 and −0.91 V versus Fc/Fc$^+$ (Fc = (η^5-C_5H_5)$_2$Fe) which are positively shifted by as much as 0.55 and 0.84 V, respectively, from that of **0Ni** (−1.75 V). The first oxidation potentials of **1Ni** and **2Ni** are also shifted and observed at 0.41 and 0.30 V, respectively, a result of the π-extension. These data led to the estimation of electrochemical HOMO–LUMO gaps of **1Ni** and **2Ni** to be 1.61 and 1.21 eV, respectively, which are roughly consistent with the optical HOMO–LUMO gaps of 1.54 and 1.22 eV.

Density functional theory (DFT) calculations have predicted that the energy levels of the degenerated HOMOs of **1Ni** are almost unchanged from those of **0Ni** (Figure 3). In contrast, the LUMO of **1Ni** is delocalized over the whole π-system and its energy is dramatically lowered to be −2.78 eV, in line with the electrochemical measurement. This is attributable to the favorable interaction between the LUMO of diphenylborane and the LUMO + 1 of the porphyrin moiety. The LUMO energy of independent diphenylborane is −2.13 eV, which is almost equal to the degenerated LUMO and LUMO + 1 energies of **0Ni** (−2.09 and −2.08 eV). Moreover, a mixing of the LUMO + 1 of the parent porphyrin and the LUMO of the diphenylborane is symmetrically favorable to construct a highly stabilized LUMO of **1Ni**. A similar orbital interaction is also observed in **2Ni**. The more stabilized LUMO of **2Ni** (−3.18 eV) is

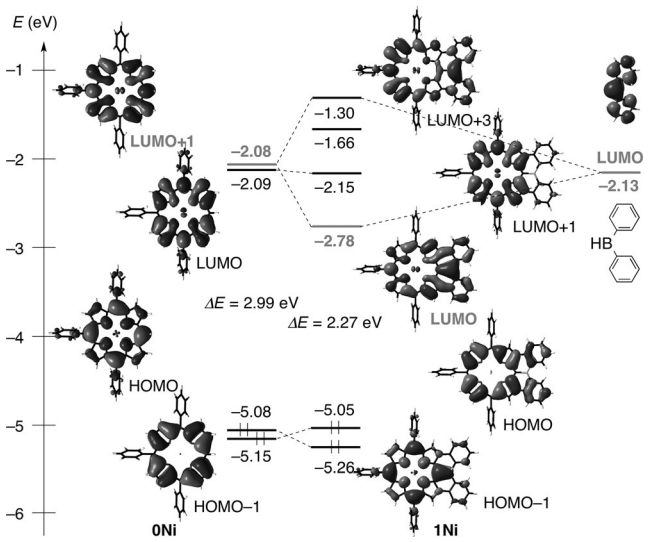

Figure 3. Energy diagrams and selected Kohn–Sham orbitals of **0Ni**, **1Ni**, and diphenylborane calculated at B3LYP/6-31G(d)/LANL2DZ level. 3,5-Di-*tert*-butylphenyl groups were replaced to phenyl groups to simplify the calculations.

constructed by a mixing between the LUMO + 1 of the parent porphyrin and the LUMO of the two diphenylboranes.

As described above, the addition of pyridine to a solution of **1M** in CH_2Cl_2 caused large spectral changes owing to the formation of adduct **1M·py**. The structures of **1Ni·py** and **1Cu·py** have been confirmed by X-ray crystallographic analysis (see Figure S25). The Lewis acidities of **1M** were evaluated by titration experiments. The titration experiment of **1Ni** is shown in Figure 4, in which the spectrum was gradually changed with clear isosbestic points at 415, 462, 518, and 614 nm. The association constant (K_a) was determined to be $1.7\times10^5\,\text{M}^{-1}$. The association constants of **$1H_2$**, **1Pd**, and **1Cu** with pyridine were also determined in a similar manner to be $3.4\times10^4\,\text{M}^{-1}$, $4.2\times10^4\,\text{M}^{-1}$, and $1.9\times10^4\,\text{M}^{-1}$ (see Figure S27), respectively. Importantly, the Lewis acidities of **1M**, as judged from the related association constants, are much higher than those of previously reported structurally constrained triarylboranes ($0.35\,\text{M}^{-1}$ in THF and $5.1\times10^3\,\text{M}^{-1}$ in toluene).[2b,g] The magnitude of the association constant with pyridine is in the order **1Ni > 1Pd > $1H_2$ > 1Cu**. To understand the origin of these different association constants, the atomic charge distributions of **1Ni**, **1Pd**, and **1Cu** have been calculated by the DFT method, which however has not revealed serious differences (see Figure S34). In addition, the electrochemical properties of **1M** revealed that the electron-accepting abilities of **1M** were independent on the inner metal (see Figure S35). Therefore, as indicated by the constrained boron compounds, the observed large association constant of **1Ni** may be a result of its conformational flexibility.[2g] The structural analyses of **1Ni·py** and **1Cu·py** also supported this tendency. In the case of structurally flexible Ni^{II} porphyrins, the MPD value is almost doubled in **1Ni·py** (being 0.311 Å), compared to **1Ni**.[12] In contrast, **1Cu·py** maintains a rigid planar porphyrin core with a small MPD value of 0.050 Å.[12]

Furthermore, we examined the coordination properties of **1Zn** bearing Lewis acidic sites on both the boron and the zinc

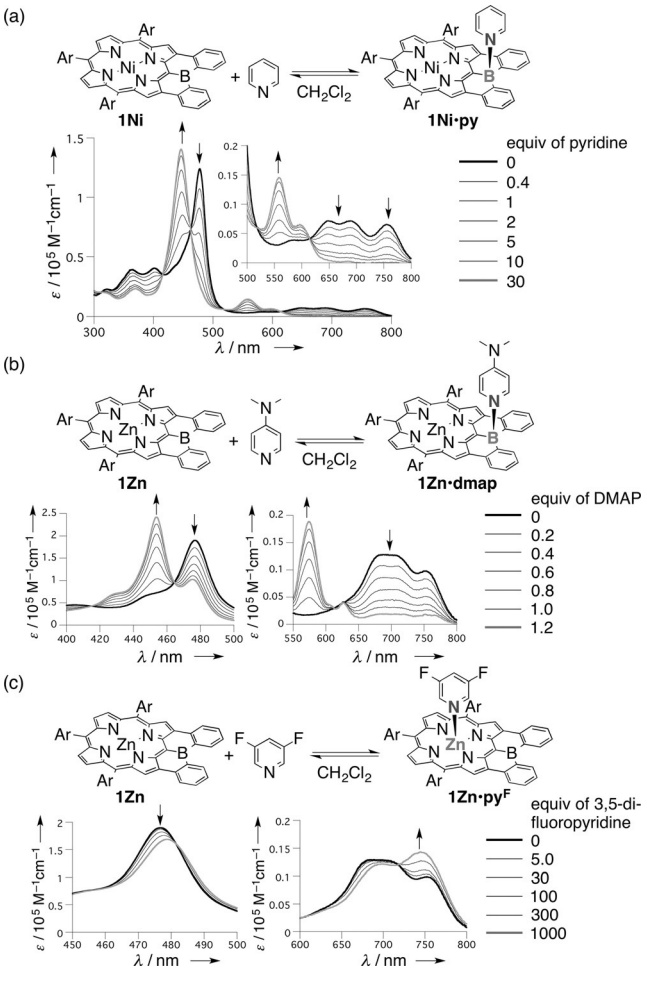

Figure 4. UV/Vis titration of a) **1Ni** with pyridine, b) **1Zn** with DMAP, and c) **1Zn** with 3,5-difluoropyridine in CH_2Cl_2 ([**1M**]$_0$: 5.0 μM).

center. Zn^{II} 5,10,15,20-tetraphenylporphyrin (ZnTPP) is known to bind pyridine at the zinc centers with an association constant of $1.1\times10^4\,\text{M}^{-1}$ in CH_2Cl_2.[13] This binding is accompanied by slight red-shifts in the Soret and Q bands in the absorption spectrum. This association constant is comparable to those of **1M** with pyridine at the boron center ($1.9–17\times10^4\,\text{M}^{-1}$). The titration experiment of **1Zn** exhibited a spectral change without any isobestic points, indicating competitive coordination of pyridine at the boron and the zinc center (see Figure S28).

On the other hand, 4-dimethylaminopyridine (DMAP) and 3,5-difluoropyridine were found to coordinate regioselectively to the boron center and the zinc center of **1Zn**, respectively. Titration experiments with DMAP caused a blue shift of its Soret band from 477 nm to 454 nm, increase of the band intensity at 575 nm, and decrease of the absorbance in the range of 630 nm to 800 nm showing clear isosbestic points at 415, 465, and 534 nm (Figure 4b and S29). Considering the observed blue shift similar to **1Ni**, these results indicated the preferential formation of **1Zn·dmap**. In contrast, titration experiment with 3,5-difluoropyridine (py^F) caused slight red shifts of the Soret and Q bands. These spectral changes, which are similar to the case of ZnTPP, indicated a preferential formation of **1Zn·py^F** (Figure 4c). The different regioselec-

tivity between DMAP and 3,5-difluoropyridine suggest that the boron center is more sensitive to the basicity of the ligands. Namely, the binding constants at the boron have a stronger correlation with the ligand basicity than those at the zinc center. In the literature, the logarithm of the association constant ($\log K_a$) of ZnTPP with pyridines show a linear correlation with the pK_a of the conjugate acids of pyridines.[13c] The slope of the linear $\log K_a/pK_a$ plot, which means the susceptibility of the zinc center of ZnTPP to the ligand basicity, was calculated to be 0.236. In a similar manner, we obtained a linear $\log K_a/pK_a$ plot for **1Cu** (see Figure S31 and S32). Then, the slope of the plot was calculated to be 0.731 indicating the much higher susceptibility of the boron center of **1Cu** toward the basicity of pyridines. A similar value of 0.746 was also calculated for the previously reported non-porphyrinic constrained triarylborane.[2g]

The fluorescence spectra of $\mathbf{1H_2}$ and **1Zn** exhibited emission bands at 768 and 777 nm with relatively low quantum yields of 0.5 and 0.7%, respectively, which were clearly blue-shifted to 686 and 655 nm with increased quantum yields of 3.3 and 1.7% for $\mathbf{1H_2}$**·py** and **1Zn·2dmap**, respectively (see Figure S37). Femtosecond transient absorption (TA) measurements showed that the S_1-state lifetimes of $\mathbf{1H_2}$, **1Ni**, and **1Zn** were 370, 4.0, and 870 ps, respectively (see Figure S38), which are well-matched with their fluorescence decays (see Figure S39). In contrast, the significantly different TA spectra of their pyridine-coordinated complexes were observed with excited-state lifetimes of 5.2 and 1.5 ns for $\mathbf{1H_2}$**·py** and **1Zn·2dmap**, respectively (see Figure S41). These TA spectra and lifetimes of pyridine-coordinated complexes are almost comparable to their porphyrin analogues,[14] clearly indicating the disruption of the electronic interaction of the empty p-orbital of boron atoms with the porphyrin π-network. Collectively, these features suggest that the embedded boron atom plays an essential role in the extension of the π-system in the diphenylborane-fused porphyrins.

In summary, diphenylborane-fused porphyrins **1M** and **2Ni** were synthesized via the one-pot reaction of the **3Ni** and **4Ni** with BBr_3. These porphyrins exhibit largely red-shifted absorption bands and enhanced electron-accepting characters, owing to the effective electronic interaction between the porphyrin and the fused diphenylboranes. The high Lewis acidic character, which is dependent on the inner metal, has been confirmed. Moreover, **1Zn** displayed regioselective binding of DMAP at the boron atom and 3,5-difluoropyridine at the zinc center.

Acknowledgements

This work was supported by ACT-C, JST, and by Grants-in-Aid from MEXT (Nos.: 25107002 "Science of Atomic Layers") and from JSPS (Nos.: 25220802 (Scientific Research (S)), 24685007 (Young Scientists (A)), 26620081 (Exploratory Research)). H.Y. acknowledges Kansai Research Foundation for Technology Promotion and The Asahi Glass Foundation for financial support. K.F. acknowledges a JSPS Fellowship for Young Scientists. This research at Yonsei University supported by the by the Ministry of Science, ICT & Future, Korea through the Global Research Laboratory Program (2013K1A1A2A02050183).

Keywords: boron · Lewis acidity · porphyrin · structural constraint · π-extension

How to cite: *Angew. Chem. Int. Ed.* **2016**, *55*, 3196–3199
Angew. Chem. **2016**, *128*, 3248–3251

[1] K. Fujimoto, H. Yorimitsu, A. Osuka, *Chem. Eur. J.* **2015**, *21*, 11311.
[2] a) Z. Zhou, A. Wakamiya, T. Kushida, S. Yamaguchi, *J. Am. Chem. Soc.* **2012**, *134*, 4529; b) S. Saito, K. Matsuo, S. Yamaguchi, *J. Am. Chem. Soc.* **2012**, *134*, 9130; c) T. Kushida, Z. Zhou, A. Wakamiya, S. Yamaguchi, *Chem. Commun.* **2012**, *48*, 10715; d) T. Kushida, S. Yamaguchi, *Organometallics* **2013**, *32*, 6654; e) C. Dou, S. Saito, K. Matsuo, I. Hisaki, S. Yamaguchi, *Angew. Chem. Int. Ed.* **2012**, *51*, 12206; *Angew. Chem.* **2012**, *124*, 12372; f) T. Kushida, C. Camacho, A. Shuto, S. Irle, M. Muramatsu, T. Katayama, S. Ito, Y. Nagasawa, H. Miyasaka, E. Sakuda, N. Kitamura, Z. Zhou, A. Wakamiya, S. Yamaguchi, *Chem. Sci.* **2014**, *5*, 1296; g) K. Matsuo, S. Saito, S. Yamaguchi, *J. Am. Chem. Soc.* **2014**, *136*, 12580; h) T. Kushida, A. Shuto, M. Yoshio, T. Kato, S. Yamaguchi, *Angew. Chem. Int. Ed.* **2015**, *54*, 6922; *Angew. Chem.* **2015**, *127*, 7026.
[3] a) J. P. Lewtak, D. T. Gryko, *Chem. Commun.* **2012**, *48*, 10069; b) H. Mori, T. Tanaka, A. Osuka, *J. Mater. Chem. C* **2013**, *1*, 2500; c) T. Tanaka, A. Osuka, *Chem. Soc. Rev.* **2015**, *44*, 943.
[4] a) W. Haubold, J. Herdtle, W. Gollinger, W. Einholz, *J. Organomet. Chem.* **1986**, *315*, 1; b) D. Kaufmann, *Chem. Ber.* **1987**, *120*, 853.
[5] a) T. Hatakeyama, S. Hashimoto, S. Seki, M. Nakamura, *J. Am. Chem. Soc.* **2011**, *133*, 18614; b) H. Hirai, K. Nakajima, S. Nakatsuka, K. Shiren, J. Ni, S. Nomura, T. Ikuta, T. Hatakeyama, *Angew. Chem. Int. Ed.* **2015**, *54*, 13581; *Angew. Chem.* **2015**, *127*, 13785.
[6] K. Fujimoto, H. Yorimitsu, A. Osuka, *Org. Lett.* **2014**, *16*, 972.
[7] a) L. S. Chen, G. J. Chen, *J. Organomet. Chem.* **1980**, *193*, 283; b) L. T. Ball, G. C. Lloyd-Jones, C. A. Russell, *J. Am. Chem. Soc.* **2014**, *136*, 254.
[8] J. E. Milne, S. L. Buchwald, *J. Am. Chem. Soc.* **2004**, *126*, 13028.
[9] J. F. Blount, P. Finocchiaro, D. Gust, K. Mislow, *J. Am. Chem. Soc.* **1973**, *95*, 7019.
[10] W. R. Scheidt in *Handbook of Porphyrin Science Vol. 24* (Eds.: K. M. Kadish, K. M. Smith, R. Guilard), World Scientific Publishing, Singapore, **2012**, chap. 111.
[11] MPD represents an average of distances between each atom and a mean plane. The mean plane was defined by 38 atoms constituting the π-conjugated plane.
[12] The mean plane was defined by 24 atoms in the porphyrin skeleton. The MPD value of **1Ni** for the 24 atoms is calculated to be 0.176 Å.
[13] a) C. H. Kirksey, P. Hambright, C. B. Storm, *Inorg. Chem.* **1969**, *8*, 2141; b) C. H. Kirksey, P. Hambright, *Inorg. Chem.* **1970**, *9*, 958; c) T. Kojima, T. Nakanishi, T. Honda, R. Harada, M. Shiro, S. Fukuzumi, *Eur. J. Inorg. Chem.* **2009**, 727.
[14] a) J. Rodriguez, C. Krimaier, D. Holten, *J. Am. Chem. Soc.* **1989**, *111*, 6500; b) H.-W. Jiang, S. Ham, N. Aratani, D. Kim, A. Osuka, *Chem. Eur. J.* **2013**, *19*, 13328; c) J. Oh, H. Yoon, Y. M. Sung, P. Kang, M.-G. Choi, W.-D. Jang, D. Kim, *J. Phys. Chem. B* **2015**, *119*, 7053.

Received: December 28, 2015
Published online: January 28, 2016

